arXiv:1403.5384v1 [cs.RO] 21 Mar 2014

NuRA: Numerical Roadmap Algorithm

Reza Iraji and Hamidreza Chitsaz

***Abstract*— Motion planning has been studied for nearly four decades now. Complete, combinatorial motion planning approaches are theoretically well-rooted with completeness guarantees but they are hard to implement. Sampling-based and heuristic methods are easy-to-implement and quite simple to customize but they lack completeness guarantees. Can the best of both worlds be ever achieved, particularly for mission-critical applications such as robotic surgery, space explorations, and handling hazardous material? In this paper, we answer affirmatively to that question. We present a new methodology, NuRA, to numerically approximate the roadmap (a network of one-dimensional algebraic curves) that is computed in the complete motion planning algorithms, namely the Canny's algorithm. Our algorithm encloses the roadmap with a chain of tiny boxes each of which contains a piece of the roadmap and whose connectivity captures the roadmap connectivity. Our algorithm starts by enclosing the entire space with a box. In each iteration, remaining boxes are shrunk on all sides and then split into smaller sized boxes. Those boxes that are empty are detected in the shrink phase and removed. The algorithm terminates when all remaining boxes are smaller than an input size. Shrink operation is cast as a polynomial optimization with semialgebraic constraints, which is in turn transformed into a (series of) semidefinite programs (SDP) using the Lasserre's approach. NuRA's success is due to fast SDP solvers. To confirm the effectiveness of NuRA, the three-leaf clover planar curve and torus roadmap were computed. In both cases, NuRA completely captured the connectivity. Since boxes are independent from one another, NuRA can be parallelized particularly on GPUs.**

I. Introduction

With the advent of automated manufacturing and robotics, the field of motion planning was introduced to the scientific society by the pioneering woks of Lozano-Perez and Reif [21], [27]. A robot usually works in a 2D or 3D environment, called work space, containing obstacles. Lozano-Perez suggested that a layer of abstraction can be added by associating any motion of the robot with a path in the set of feasible distinct robot configurations, also known as the configuration space C. That association induces a natural correspondence between work space obstacles O and obstacle regions in the configuration space C_{obs}. Often, the collision-free subset of the configuration space $C_{free} = C \backslash C_{obs}$ can be explained by a set of polynomial inequalities that are computed from the description of O and robot. The input of a motion planning problem is that set of polynomial inequalities and an initial and a goal point in C_{free}.

Early in the field, the motion planning problem was proved to be PSPACE-hard and consequently NP-hard [27]. In the first attempts to solve the problem, researchers aimed at complete, combinatorial algorithms. This led to some outstanding works such as the use of Collins cylindrical algebraic decomposition by Schwartz and Sharir [9], [10], [28]–[30] and the Canny's roadmap algorithm [6].

R. Iraji and H. Chitsaz are with the Department of Computer Science, Wayne State University, 5057 Woodward Ave Suite 3010, Detroit, MI {iraji, chitsaz}@wayne.edu

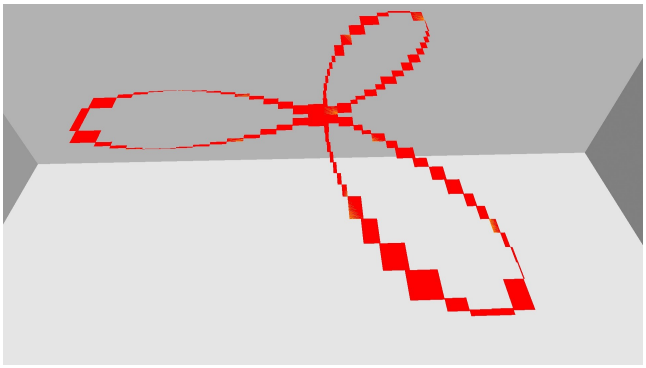

Three-leaf clover planar curve

Fig. 1. A boxified three-leaf clover planar curve in $\mathbb{R}^3$.

Schwartz and Sharir gave the first complete motion planning algorithm for a rigid body in two and three dimensions [28]–[30]. Their algorithm is based on algebraic geometry methods, specifically cylindrical algebraic decomposition [9], [10]. The running time of Schwartz-Sharir algorithm is doubly-exponential in the dimension of the configuration space. Canny introduced a singly exponential time complexity algorithm based on the Morse theory and resultants in commutative algebra, which is near optimal provided $P \neq NP$. Recently, the Canny's algorithm was improved by Basu *et al.* [1]–[3]. Safey El Din and Schost have embarked on a journey to achieve the optimal roadmap algorithm by a (nearly) balanced division of dimension at each recursive iteration of the algorithm [11].

Although the Canny's algorithm was the theoretical bottom line, it was of little use in practice since implementing it involved an unmanageable level of sophistication. To the best of our knowledge, there is still no publicly available implementation of the roadmap algorithm to date. That fact inspired another trend in the field in the 1990s to address practical motion planning problems. Discretization and grid search were among the first attempts along those lines [7], [17]. Numerous easy-to-implement heuristic approaches such as artificial potential fields [12], [13], [15], [20] and sampling-based motion planning algorithms that claim probabilistic completeness [14], [19] have appeared.

For some non-critical applications, sampling-based motion planning algorithms have proven to be applicable in practice.

However, one cannot use a heuristic motion planner for robotic surgery, space explorations, nuclear facility repair, and handling life-threatening material among many mission critical applications. We conjecture that if robots are to ubiquitously enter our day-to-day lives, they have to be equipped with advanced, theoretically well-rooted motion planners with some form of completeness guarantee.

At the first glance, the requirement of both completeness and practicality of solution may appear unattainable. Complete general motion planning algorithms, namely cylindrical algebraic decomposition and the roadmap algorithm, are based on real algebraic geometry computations which is extremely difficult to implement. Although the problem was theoretically solved by the Canny's innovative algorithm, it remains open from a practical perspective. The reason is that solving the Canny's polynomial system of equations is intractable symbolically. More precisely, simplifying that system of equations into one polynomial equation, called the resultant, is very hard.

Furthermore, even though sampling-based motion planning algorithms became popular due to solving the problem for some non-critical applications, they never met the reliability expectations for mission-critical applications. The convergence rate of sampling-based algorithms is low in the case of narrow passages, which occur frequently in real world. Sampling-based algorithms often waste computation on the wrong part of a problem, namely narrow passages that do not even cause NP-hardness [31]. Also, local approaches such as artificial potential field suffer from getting trapped in local minima. Dealing with this problem, either by designing a navigation function which guarantees no local minima [8] or by heuristic approaches [13], makes the problem so complicated that sometimes cannot be solved at all or makes it unreliable and consequently unsuitable for mission-critical applications.

Despite decades of research in motion planning, there is still a gap in the field. To fill this gap, we introduce a new methodology, inspired by the roadmap algorithms, in this paper to simultaneously maintain both completeness and practicality for a large class of problems.

II. Problem

We consider the problem of planning motion for robotic systems. Each robot is composed of arbitrary open/closed kinematic chains of bodies (generally semialgebraic objects). Two objects are in collision if their surfaces are closer than d in the Euclidean space. Mathematically, the space of collision-free configurations of the entire system of robots (C_{free}) can be represented by a semialgebraic set

$$S := \{x \in \mathbb{R}^n \mid f_1(x) \geq 0, f_2(x) \geq 0, \ldots, f_m(x) \geq 0\}, \tag{1}$$

in which $f_i \in \mathbb{R}[X]$ are polynomials. Note that S is parametrized by d, but for the sake of brevity we do not explicitly denote it in this paper. We denote $X_1, X_2, \ldots, X_n$ variables by X (see Chapter 2 of [6] for a detailed derivation of f polynomials). We are given the f_i polynomials and the initial configuration x_I and the goal configuration x_G in S. The motion planning problem asks for a path in S from x_I to x_G if there is such a path and non-existence report otherwise. The Canny's roadmap algorithm computes a one-dimensional semialgebraic subset of S, called the roadmap, and pieces of semialgebraic curves connecting x_I and x_G to the roadmap. A graph connectivity query from x_I to x_G then yields the result. Since the roadmap is guaranteed to cross every Morse slice of the configuration space, it essentially captures the topology of the space.

Our idea is to approximate edges of the roadmap, which are algebraic curves implicitly defined as the zero set of a system of polynomials, by chains of adjacent bounding boxes in $\mathbb{R}^n$, each of which contains a slice of the roadmap. Faces of such bounding boxes are computed by iterative polynomial optimization on semialgebraic sets [18], [32] which are performed in turn by a series of semidefinite programs (SDP) [33]. Our approach is in the spirit of Porta's *et al.* [24], [25], albeit using a more sophisticated SDP-based optimization on the roadmap.

The roadmap algorithm consists of computing the roadmap for real algebraic varieties

$$g(x) = f_{i_1}(x)^2 + f_{i_2}(x)^2 + \cdots + f_{i_k}(x)^2 = 0, \tag{2}$$

where $1 \leq k \leq \ell \leq m$ and ℓ is the Basu-Pollack-Roy complexity of S [1], and $\{i_1, i_2, \ldots, i_k\}$ ranges over all possible k-element subsets of $\{1, 2, \ldots, m\}$. These individual roadmaps are then connected along their intersections with other varieties to form the global roadmap of S. In reality, many of these varieties are empty in which case their roadmap is just empty. Our numerical algorithm detects such cases in the first step, which will cause the expected number of considered varieties in our algorithm much lower than the worst case exponential m^ℓ. Moreover, modern collision detection techniques [23] provide valuable information that can help detect such empty varieties beforehand. In the following, the approach is presented in more detail.

III. Approach

There are two types of objects that are approximated numerically in our work: curves and points. Curves, which are edges of the roadmap mainly captured in the skeleton (see below), are represented by a chain of adjacent bounding boxes [25]. A point is represented by one bounding box. Both curves and points arise as the zero sets of systems of polynomials that are computed in the roadmap algorithm. We first explain below how those systems of polynomials are computed, which is taken from the roadmap algorithm. We then explain how we approximate a one or zero dimensional zero set of a system of polynomials. Note that our approximation scheme preserves completeness of the roadmap algorithm.

A. Skeleton

Within the core of the roadmap algorithm lies computation of the skeleton, which is the preimage of the silhouette of the projection of the input variety (2) onto the first

two coordinates. More precisely, the skeleton is the first approximation of

$$\Sigma(\epsilon) := \{x \in \mathbb{R}^n \mid g(x) = \epsilon, \frac{\partial g}{\partial x_3} = 0, \ldots, \frac{\partial g}{\partial x_n} = 0\}, \quad (3)$$

as $\epsilon \to 0$. The roadmap algorithm treats ϵ as a variable and employs elimination theory to compute a resultant polynomial $h \in \mathbb{R}[X_1, X_2, \epsilon]$ such that

$$\Sigma(\epsilon) = \{x \in \mathbb{R}^n \mid g(x) = \epsilon, h(x_1, x_2, \epsilon) = 0\}. \quad (4)$$

The zero set of the coefficients of the lowest degree ϵ in $h(x_1, x_2, \epsilon)$ together with $g(x) = 0$ define Σ. Our method is much easier to implement since we will use numerical calculations instead of computer algebra. For more general cases, advanced multi-infinitesimal-based algebraic methods have been given to compute the roadmap skeleton [1].

B. Points

A point $A \in S$ is called X_1-critical if $\frac{\partial g}{\partial x_2}|_A = 0$. In the roadmap algorithm [6], recursive calls to the skeleton algorithm are performed on the slices of S at X_1-critical points. In other parts of the roadmap algorithm, intersections of Σ with other varieties, which are gluing vertices of the roadmap, are computed.

For all those points, our algorithm computes a bounding box, instead of an exact algebraic point (zero set of a resultant polynomial), using Newton method. For instance, bounding boxes are computed by intersecting the chain of bounding boxes in Σ with the variety in the other leg of intersection.

C. Lazy Recursions

Those recursive calls to the skeleton algorithm are slightly more complicated in our case. Let $A = (a_1, a_2, \ldots, a_n) \in \mathbb{R}^n$ be an X_1-critical point. The Canny's algorithm calls the skeleton algorithm on $S \cap \{x \in \mathbb{R}^n \mid x_1 = a_1\}$ slice of S. Our algorithm does not compute A precisely, but it rather approximates A numerically by a bounding box $[a_1^l, a_1^u] \times \cdots \times [a_n^l, a_n^u] \ni A$. At what slice should the roadmap algorithm be recursively called?

The skeleton algorithm is called twice: once for the lower slice $S \cap \{x \in \mathbb{R}^n \mid x_1 = a_1^l\}$, and once for the upper slice $S \cap \{x \in \mathbb{R}^n \mid x_1 = a_1^u\}$. Both skeletons are then added to the roadmap. This approach imposes a constant running time overhead but guarantees completeness of the algorithm. The Morse theorem shows that the topology of X_1-slices do not change between consecutive X_1-critical values [6]. Hence, our algorithm guarantees completeness provided that exactly one X_1-critical value is contained within $[a_1^l, a_1^u]$ interval, which is a matter of resolution.

After completion of each recursive call to the skeleton algorithm, our algorithm searches the partially built roadmap to see if it finds a path from x_I to x_G in the roadmap. Often, a path may appear in partially built roadmaps, in which case our algorithm will not continue recursions further on X_1-critical intervals and will save computation time.

D. Bounding Boxes

Given a skeleton piece (point) of the roadmap, which is a one (zero) dimensional real variety in S,

$$Z := S \cap \{x \in \mathbb{R}^n \mid h_1(x) = 0, h_2(x) = 0, \ldots, h_k(x) = 0\}, \quad (5)$$

our algorithm computes a set of sufficiently small boxes B that contain Z, i.e. $Z \subset \bigcup_{b \in B} b$. The algorithm starts with an initial box set

$$B = \Big\{[l_1, u_1] \times [l_2, u_2] \times \cdots \times [l_n, u_n]\Big\}, \quad (6)$$

containing the entire configuration space $S \subset [l_1, u_1] \times [l_2, u_2] \times \cdots \times [l_n, u_n]$. Non-compact configuration spaces can be compactified; hence, we assume S is compact, in which case there is such an initial bounding box. Our algorithm iterates over two operations, *shrinking* and *splitting*, on bounding boxes in B. Shrinking eliminates portions of a box that do not contain any piece of the variety, and box splitting refines the resolution. This iterative process continues until all boxes are either empty or sufficiently small. Our algorithm is inherently multi-resolution, which means the termination criteria can be evaluated box by box, locally based on neighboring boxes, root separations, and also based on criticality of the application.

1) Box Shrinking: Given a box $b = [l_1, u_1] \times [l_2, u_2] \times \cdots \times [l_n, u_n]$, this module of the algorithm squeezes b to obtain the smallest box $b' = [l_1', u_1'] \times [l_2', u_2'] \times \cdots \times [l_n', u_n'] \subseteq b$ that contains $Z \cap b$. Our algorithm iteratively shrinks the interval of each dimension until no more shrinking is possible. Here, we present our algorithm to shrink $[l_i, u_i]$ to obtain $[l_i'', u_i'']$. Note that we cannot necessarily obtain $[l_i', u_i']$ in one step, and the algorithm iterates potentially multiple times over shrinking every dimension. However, the algorithm is able to discover empty boxes in one iteration.

Shrinking $[l_i, u_i]$ to obtain $[l_i'', u_i'']$ is cast as the following optimization problems

$$\begin{aligned} l_i'' = \underset{x}{\text{minimize}} \quad & x_i \\ u_i'' = \underset{x}{\text{maximize}} \quad & x_i \\ \text{subject to} \quad & l_j \le x_j \le u_j,\ 1 \le j \le n, \\ & h_j(x) = 0,\ 1 \le j \le k, \\ & f_j(x) \ge 0,\ 1 \le j \le m, \\ & \left\lceil \sum_{j=1}^{n} l_j^2 + u_j^2 \right\rceil - \sum_{j=1}^{n} x_j^2 \ge 0, \end{aligned} \quad (7)$$

where the constraints correspond to the current bounding box, the input semialgebraic set (5), and satisfaction of a technical assumption. We propose to solve these optimization problems using the Lasserre's approach [18], [32] which requires satisfaction of a general assumption described below in (19) [32]. That is why we added the last constraint above. Obviously, the last constraint does not affect the result. For

the sake of presentation, let

$$c = 2n + 2k + m + 1, \tag{8}$$
$$Z_b = Z \cap b, \tag{9}$$
$$e_0(x) = 1, \tag{10}$$
$$e_j(x) = x_j - l_j,\ 1 \le j \le n, \tag{11}$$
$$e_{n+j}(x) = u_j - x_j,\ 1 \le j \le n, \tag{12}$$
$$e_{2n+j}(x) = h_j(x),\ 1 \le j \le k, \tag{13}$$
$$e_{2n+k+j}(x) = -h_j(x),\ 1 \le j \le k, \tag{14}$$
$$e_{2n+2k+j}(x) = f_j(x),\ 1 \le j \le m, \tag{15}$$
$$e_{2n+2k+m+1}(x) = \left\lceil \sum_{j=1}^{n} l_j^2 + u_j^2 \right\rceil - \sum_{j=1}^{n} x_j^2. \tag{16}$$

Using this notation, (7) becomes

$$\begin{aligned} l_i'' = \underset{x}{\text{minimize}} \quad & x_i \\ u_i'' = \underset{x}{\text{maximize}} \quad & x_i \\ \text{subject to} \quad & e_j(x) \ge 0,\ 1 \le j \le c. \end{aligned} \tag{17}$$

Denote the set of all squares p^2 of polynomials $p \in \mathbb{R}[X]$ by $\mathbb{R}[X]^2$, the set of all $p^2 e_j$ by $\mathbb{R}[X]^2 e_j$, and the set of all finite sums of such elements by $\sum \mathbb{R}[X]^2 e_j$. The set

$$\begin{aligned} M &:= \sum \mathbb{R}[X]^2 + \sum \mathbb{R}[X]^2 e_1 + \cdots + \sum \mathbb{R}[X]^2 e_c \\ &= \left\{ \sum_{j=0}^{c} q_j e_j \;\middle|\; q_j \in \sum \mathbb{R}[X]^2 \right\}, \end{aligned} \tag{18}$$

is the quadratic module generated by $e_1, \ldots, e_c$. Note that addition of $e_c(x) \ge 0$ to the constraints helps satisfy the Lasserre's general assumption [32]:

$$\exists N \in \mathbb{N} : N - \sum_{i=1}^{n} X_i^2 \in M, \tag{19}$$

with $N = \left\lceil \sum_{j=1}^{n} l_j^2 + u_j^2 \right\rceil$. The Lasserre's method convexifies the problem in two different ways. The first one is to exchange the points of the underlying feasible semialgebraic set Z_b by probability measures on Z_b. Every point $x \in Z_b$ can be identified with the Dirac measure δ_x at x. Therefore, (17) is equivalent to

$$\begin{aligned} l_i'' &= \inf \left\{ \int x_i d\mu \;\middle|\; \mu \in \mathcal{M}^1(Z_b) \right\}, \\ u_i'' &= \sup \left\{ \int x_i d\mu \;\middle|\; \mu \in \mathcal{M}^1(Z_b) \right\}, \end{aligned} \tag{20}$$

in which $\mathcal{M}^1$ denotes the set of probability measures. The second method of convexification is to cast the dual problems as

$$\begin{aligned} l_i'' &= \sup \{ a \in \mathbb{R} \mid x_i - a > 0 \text{ on } Z_b \}, \\ u_i'' &= \inf \{ a \in \mathbb{R} \mid x_i - a < 0 \text{ on } Z_b \}. \end{aligned} \tag{21}$$

For the sake of brevity, we continue presenting our approach only for the lower bound l_i''. For the upper bound, we will use the obvious analogue. Using Putinar's *Positivstellensatz* theorems [26], (20) becomes

$$\begin{aligned} l_i'' = \inf \{ L(X_i) \mid L : \mathbb{R}[X] \to \mathbb{R} \text{ is linear, } L(1) = 1, \\ L(M) \subseteq [0, \infty) \}, \end{aligned} \tag{22}$$

and (21) becomes

$$l_i'' = \sup \{ a \in \mathbb{R} \mid X_i - a \in M \}. \tag{23}$$

The idea is to relax (22) and (23) by approximations $M_d \subseteq \mathbb{R}[X]_d$ of $M \subseteq \mathbb{R}[X]$, in which $\mathbb{R}[X]_d$ denotes the vector space of polynomials $p \in \mathbb{R}[X]$ of degree at most d. More precisely,

$$\begin{aligned} M_d &:= \sum \mathbb{R}[X]_{d_0}^2 + \sum \mathbb{R}[X]_{d_1}^2 e_1 + \cdots + \sum \mathbb{R}[X]_{d_c}^2 e_c \\ &= \left\{ \sum_{j=0}^{c} q_j e_j \;\middle|\; q_j \in \sum \mathbb{R}[X]^2,\ \deg(q_j e_j) \le d \right\}. \end{aligned} \tag{24}$$

Above,

$$d \ge \max\{\deg e_1, \ldots, \deg e_c, 1\}, \tag{25}$$
$$d_j := \max\{w \in \mathbb{N} \mid 2w + \deg e_j \le d\}. \tag{26}$$

Replacing M by M_d, we obtain the following pair of primal-dual optimization problems

$$\begin{aligned} (P_d) \quad & \text{minimize} \quad & & L(X_i) \\ & \text{subject to} \quad & & L : \mathbb{R}[X]_d \to \mathbb{R} \text{ is linear}, \\ & & & L(1) = 1, \\ & & & L(M_d) \subseteq [0, \infty), \\ (D_d) \quad & \text{maximize} \quad & & a \\ & \text{subject to} \quad & & a \in \mathbb{R}, \\ & & & X_i - a \in M_d. \end{aligned}$$

Denoting the solution of (P_d) by P_d^* and that of (D_d) by D_d^*, the Lasserre's theorem [18] guarantees that $\{D_d^*\}$ and $\{P_d^*\}$ are increasing sequences that converge to l_i'' and satisfy $D_d^* \le P_d^* \le l_i''$. This property is an important feature of our algorithm. In fact, l_i'' is a mere lower bound for the bounding box. The tighter the better, but it should not be overestimated as some parts of the roadmap will remain uncontained in that case. The fact that our consecutive approximations converge from below to l_i'' assures that l_i'' will never be overestimated. The analogous property guarantees that u_i'' will not be underestimated.

We solve these optimization problems by transforming them into semidefinite programs. We denote the set of possible monomial exponent vectors with total degree not more than d by

$$\mathcal{E}(d) := \{\alpha \in (\mathbb{N} \cup \{0\})^n \mid |\alpha|_1 \le d\}, \tag{27}$$

the exponent vector of X_i by

$$\iota = (0, \ldots, \iota_i = 1, \ldots, 0), \tag{28}$$

the set of symmetric *positive semidefinite* $r \times r$ matrices by $\mathbb{R}^{r\times r}_{s+}$, and the inner product of two $r \times r$ matrices A and B by

$$\langle A, B\rangle := \sum_{j,l=1}^{r} A(j,l)B(j,l). \tag{29}$$

Define matrices $A_{\alpha j} \in \mathbb{R}^{|\mathcal{E}(d_j)|\times|\mathcal{E}(d_j)|}_{s+}$ for $j \in \{0,\ldots,c\}$ and $\alpha \in \mathcal{E}(d)$ implicitly by

$$X^{\beta+\gamma}e_j = \sum_{\alpha\in\mathcal{E}(d)} A_{\alpha j}(\beta,\gamma)X^{\alpha}, \tag{30}$$

for $\beta,\gamma \in \mathcal{E}(d_j)$. Simply, $A_{\alpha j}(\beta,\gamma)$ is the coefficient of X^{α} in $X^{\beta+\gamma}e_j$. In that case, (P_d) and (D_d) become the following pair of primal-dual semidefinite programs:

$$\begin{aligned}
(P^{\text{sdp}}_d) \quad \text{minimize} \quad & \sum_{j=0}^{c}\langle A_{0j}, Q_j\rangle \\
\text{subject to} \quad & Q_j \in \mathbb{R}^{|\mathcal{E}(d_j)|\times|\mathcal{E}(d_j)|}_{s+}, \\
& \sum_{j=0}^{c}\langle A_{\iota j}, Q_j\rangle = 1, \\
& \sum_{j=0}^{c}\langle A_{\alpha j}, Q_j\rangle = 0,\ \alpha \in \mathcal{E}(d)\backslash\{0,\iota\}, \\
(D^{\text{sdp}}_d) \quad \text{maximize} \quad & y_{\iota} \\
\text{subject to} \quad & y_{\alpha} \in \mathbb{R},\ 0 \neq \alpha \in \mathcal{E}(d), \\
& A_{0j} - \sum_{\alpha\in\mathcal{E}(d)\backslash\{0\}} y_{\alpha}A_{\alpha j} \ \text{ is positive} \\
& \qquad \text{semidefinite},\ j \in \{0,\ldots,c\}.
\end{aligned}$$

2) Box Splitting: The algorithm splits a box through dividing its largest interval at the point that yielded the optimal value in the box shrinking optimization above if that point is in the interior. Otherwise, the algorithm splits a box through halving its largest interval.

IV. Results

A. Implementation

The algorithm was written in C++. OpenGL was utilized to visualize the output of the program. For solving semidefinite programs to shrink the boxes, there are efficient open source semidefinite programming packages such as SDPA [16], SDPARA [34], SDPARA-C [22], CSDP [5], and DSDP [4]. For convenience, we used CSDP [5] in our implementation that is capable of solving problems of the form

$$\begin{aligned}
\text{maximize} \quad & tr(CX) \\
\text{subject to} \quad & tr(A_iX) = a_i,\ 1 \leq i \leq m \\
& X \in \mathbb{R}^{r\times r}_{s+},
\end{aligned}$$

where all the A_i, X, and C are real and symmetric $r \times r$ matrices.

CSDP has a special, fast treatment of block diagonal matrices. Fortunately, the finalized semidefinite program in Section III-D.1 is in fact a program with matrices in block diagonal structure. Therefore, the primal semidefinite program, which is fed into CSDP, is

$$\begin{aligned}
\text{maximize} \quad & \langle A_0, Q\rangle \\
\text{subject to} \quad & \langle A_{\iota}, Q\rangle = 1, \\
& \langle A_{\alpha}, Q\rangle = 0,\ \alpha \in \mathcal{E}(d)\backslash\{0,\iota\}, \\
& Q \in \mathbb{R}^{r\times r}_{s+},
\end{aligned}$$

where for each $\beta \in \mathcal{E}(d)$, A_{β} consists of $c+1$ diagonal blocks $A_{\beta j}$, $j \in \{0,\ldots,c\}$.

It has been shown that P^*_d and D^*_d converge rapidly to the solution in practice. Moreover, we only require a lower bound for l''_i (upper bound for u''_i), not necessarily the optimal value. Hence, although the size of these programs are exponential in the dimension, i.e. $|\mathcal{E}(d)|$ is $O(d^n)$, we expect to solve these optimizations only for few small d. Moreover, as mentioned before, $A_{\beta j}$ are sparse in practice and may be grouped to simplify these programs using the special structure of (2), (3), and (10)-(16).

B. Experiments

We used our algorithm on two test cases: (i) three-leaf clover planar curve embedded in $\mathbb{R}^3$, and (ii) the Canny's roadmap for the torus. Fig. 1 depicts the boxes that enclose the clover curve, and Fig. 2 shows the boxes that contain the Canny's roadmap skeleton, recursion, and their union. In both test cases, boxes were refined until their longest side was no longer than 0.1.

The three-leaf clover curve, defined in (31), was used to confirm that our algorithm works correctly on any algebraic curve, the special case of which is Canny's roadmap skeleton. The algorithm was able to capture its connectivity.

$$(x^2+y^2)^2 - x^3 + 3xy^2 = 0. \tag{31}$$

Canny's standard example in his dissertation was the torus roadmap [6]. We chose that as the second test case. In this case too, the roadmap connectivity was preserved. The considered torus was

$$36(x^2+y^2) - (5+x^2+y^2+z^2)^2 = 0, \tag{32}$$

with radii 3 and 2.

We ran our code on a single AMD Opteron 6180 SE 2.5 GHz core. Table I shows the number of boxes and running time in each case. Note that the running time reported in Table I is without any effort to parallelize the code. Using GPUs, we expect to achieve a significant speedup as the computations for each box are independent from those for another box, and hence, NuRA can be parallelized in a relatively straight forward manner.

TABLE I. The number of boxes and running time for the clover curve and the torus skeleton and recursion.

Case	Boxes	Time (s)	Time per box (s)
Clover	94	67	0.71
Torus Skeleton	492	411	0.84
Torus Recursion	668	477	0.71

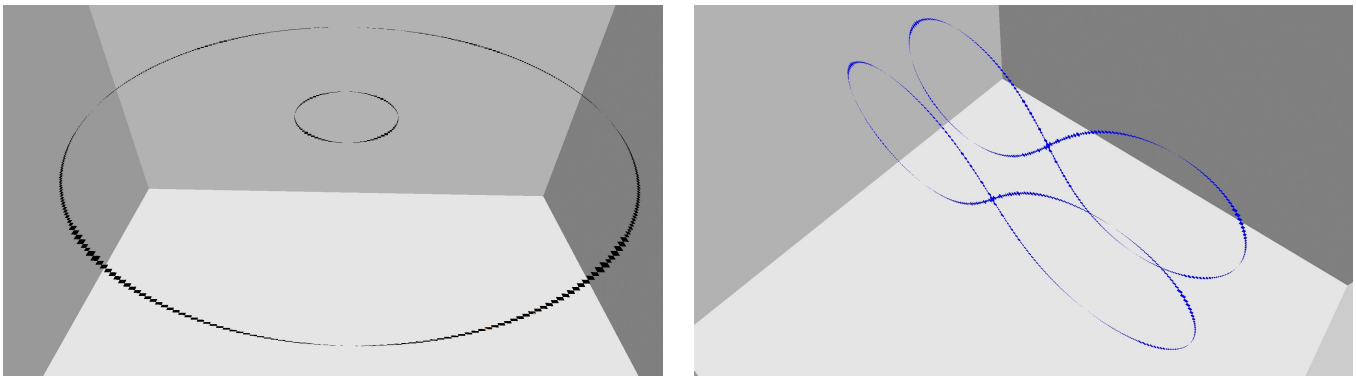

Skeleton Recursion

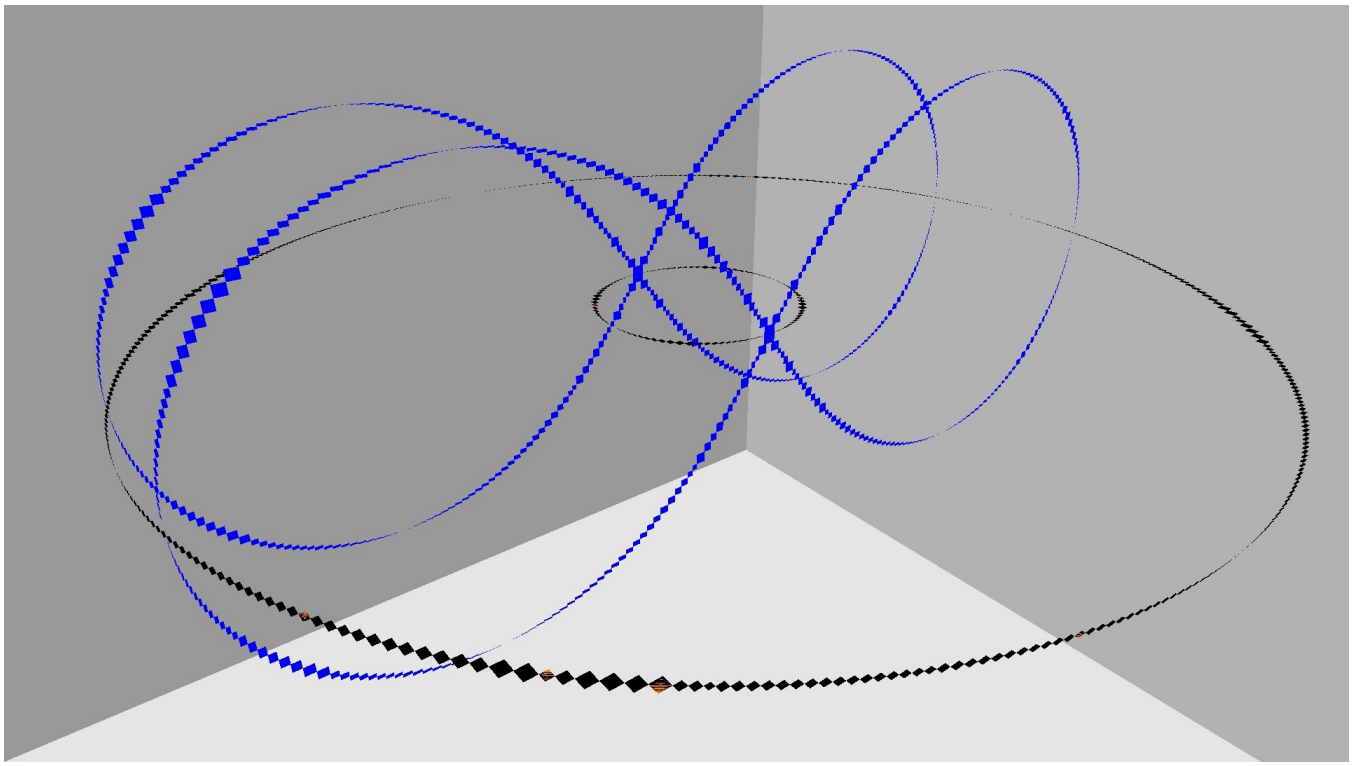

Roadmap

Fig. 2. The skeleton and recursion portions of the torus roadmap (top) and the torus roadmap (bottom).

V. Conclusions

Complete, combinatorial motion planning approaches are theoretically well-endowed with elegant completeness guarantees but they are practically useless while sampling-based and heuristic methods are easy-to-implement and quite simple to customize and add more heuristic features one on top of another but they lack completeness guarantees. Can the best of both worlds be ever achieved?

In this paper, we tried to answer affirmatively to that question. Our proposed methodology, NuRA, tries to utilize the strengths and compensate the weaknesses of the previous approaches to introduce a reliable, practical method to solve the motion planning problems for real applications, specially the mission-critical ones. In order to confirm the effectiveness of NuRA, a number of experiments were done. The simulation results suggest that NuRA can be considered as an influential progress in motion planning since

- NuRA guarantees the whole roadmap is captured even though it is approximated. Therefore, it is resolution complete.
- NuRA can be customized for a particular application accuracy and computational intensity requirements by setting the resolution parameter: the higher the resolution, the more details of roadmap is captured.
- NuRA can be highly parallelized, particularly on GPUs, which makes it deployable on embedded devices.

In summary, NuRA satisfies both completeness and practicality characteristics making it very efficacious as an emerg-

ing state-of-the-art approach.

REFERENCES

[1] S. Basu, R. Pollack, and M.-F. Roy. Computing roadmaps of semi-algebraic sets on a variety. *J. American Math. Soc.*, 13(1):55–82, 2000.

[2] S. Basu, R. Pollack, and M.-F. Roy. *Algorithms in Real Algebraic Geometry*. Springer, 2006.

[3] S. Basu, M-F. Roy, M. Safey El Din, and éE. Schost. A baby step-giant step roadmap algorithm for general algebraic sets. *arXiv preprint arXiv:1201.6439*, 2012.

[4] Steven J. Benson, Yinyu Ye, and Xiong Zhang. Solving large-scale sparse semidefinite programs for combinatorial optimization. *SIAM J. Optimization*, 10(2):443–461, 2000.

[5] B. Borchers and J.G. Young. Implementation of a primal–dual method for SDP on a shared memory parallel architecture. *Computational Optimization and Applications*, 37(3):355–369, 2007.

[6] J. F. Canny. *The Complexity of Robot Motion Planning*. MIT Press, Cambridge, MA, 1988.

[7] P.C. Chen and Y.K. Hwang. Sandros: A motion planner with performance proportional to task difficulty. In *Proc. of IEEE Int. Conf. Robotics and Automation*, pages 2346–2353, Nice, France, 1992.

[8] H. Choset, K. Lynch, S. Hutchinson, G. Kantor, W. Burgard, L. Kavraki, and S. Thrun. *Principles of Robot Motion: Theory, Algorithms and Implementation*. MIT Press, 2005.

[9] G. E. Collins. Quantifier elimination for the elementary theory of real closed fields by cylindrical algebraic decomposition. In *Lecture Notes in Computer Science*, volume 33, pages 134–183. Springer-Verlag, Berlin, 1975.

[10] George E. Collins. Quantifier elimination for real closed fields by cylindrical algebraic decomposition: a synopsis. *SIGSAM Bull.*, 10(1):10–12, February 1976.

[11] Mohab Safey El Din and Éric Schost. A nearly optimal algorithm for deciding connectivity queries in smooth and bounded real algebraic sets. *CoRR*, abs/1307.7836, 2013.

[12] R. Iraji and M. T Manzuri-Shalmani. AMF: A novel reactive approach for motion planning of mobile robots in unknown dynamic environments. In *Robotics and Biomimetics (ROBIO), 2009 IEEE International Conference on*, pages 1698–1703, Dec 2009.

[13] R. Iraji and M.T. Manzuri-Shalmani. A new fuzzy-based spatial model for robot navigation among dynamic obstacles. In *Control and Automation, 2007. ICCA 2007. IEEE International Conference on*, pages 1323–1328, May 2007.

[14] L. E. Kavraki. *Random Networks in Configuration Space for Fast Path Planning*. PhD thesis, Stanford University, 1994.

[15] O. Khatib. Real-time obstacle avoidance for manipulators and mobile robots. *Int. J. Robot. Res.*, 5(1):90–98, 1986.

[16] Sunyoung Kim, Masakazu Kojima, Martin Mevissen, and Makoto Yamashita. Exploiting sparsity in linear and nonlinear matrix inequalities via positive semidefinite matrix completion. *Math. Program.*, 129(1):33–68, September 2011.

[17] K. Kondo. Motion planning with six degrees of freedom by multistrategic bidirectional heuristic free-space enumeration. *IEEE Transactions on Robotics and Automation*, 7(3):267–277, 1991.

[18] Jean B. Lasserre. Global optimization with polynomials and the problem of moments. *SIAM J. Optimization*, 11:796–817, 2001.

[19] Steven M. Lavalle, James J. Kuffner, and Jr. Rapidly-exploring random trees: Progress and prospects. In *Algorithmic and Computational Robotics: New Directions*, pages 293–308, 2000.

[20] S. G. Loizou, D. V. Dimarogonas, and K. J. Kyriakopolous. Decentralized feedback stabilization of multiple nonholonomic agents. In *Proceedings IEEE International Conference on Robotics and Automation*, 2004.

[21] Tomás Lozano-Pérez and Michael A. Wesley. An algorithm for planning collision-free paths among polyhedral obstacles. *Commun. ACM*, 22(10):560–570, October 1979.

[22] Kazuhide Nakata, Makoto Yamashita, Katsuki Fujisawa, and Masakazu Kojima. A parallel primal-dual interior-point method for semidefinite programs using positive definite matrix completion. *Parallel Comput.*, 32(1):24–43, January 2006.

[23] Jia Pan, Sachin Chitta, and Dinesh Manocha. FCL: a general purpose library for collision and proximity queries. In *Proceedings IEEE International Conference on Robotics and Automation*, pages 3859–3866, 2012.

[24] J. M. Porta, L. Ros, F. Thomas, F. Corcho, J. Canto, and J. J. Perez. Complete maps of molecular-loop conformational spaces. *J Comput Chem*, 28(13):2170–2189, Oct 2007.

[25] Josep M. Porta, Lluís Ros, and Federico Thomas. A linear relaxation technique for the position analysis of multiloop linkages. *IEEE Transactions on Robotics*, 25(2):225–239, April 2009.

[26] M. Putinar. Positive polynomials on compact semi-algebraic sets. *Indiana University Mathematics Journal*, 42(3):969–984, 1993.

[27] J. H. Reif. Complexity of the mover's problem and generalizations. In *Proc. of IEEE Symp. on Foundat. of Comp. Sci.*, pages 421–427, 1979.

[28] J. T. Schwartz and M. Sharir. On the piano movers' problem: I. The case of a two-dimensional rigid polygonal body moving amidst polygonal barriers. *Communications on Pure and Applied Mathematics*, 36:345–398, 1983.

[29] J. T. Schwartz and M. Sharir. On the piano movers' problem: II. General techniqies for computing topological properties of algebraic manifolds. *Advances in applied Mathematics*, 4(3):298–351, 1983.

[30] J. T. Schwartz and M. Sharir. On the piano movers' problem: III. Coordinating the motion of several independent bodies. *Int. J. Robot. Res.*, 2(3):97–140, 1983.

[31] Jacob T. Schwartz, Micha Sharir, and John E. Hopcroft, editors. *Planning, geometry, and complexity of robot motion*. Ablex Publishing Corp., Norwood, NJ, USA, 1986.

[32] Markus Schweighofer. Optimization of polynomials on compact semialgebraic sets. *SIAM J. Optimization*, 15(3):805–825, March 2005.

[33] Lieven Vandenberghe and Stephen Boyd. Semidefinite programming. *SIAM Review*, 38:49–95, 1994.

[34] Makoto Yamashita, Katsuki Fujisawa, Mituhiro Fukuda, Kazuhide Nakata, and Maho Nakata. Algorithm 925: Parallel solver for semidefinite programming problem having sparse schur complement matrix. *ACM Trans. Math. Softw.*, 39(1):6:1–6:22, November 2012.